Research Article Vol. 30, No. 15 / 18 Jul 2022 / Optics Express 26886
Optics EXPRESS

Heterogeneous multicore fiber-based microwave frequency measurement

ELHAM NAZEMOSADAT,* SERGI GARCÍA, AND IVANA GASULLA

ITEAM Research Institute, Universitat Politècnica de València, Camino de Vera, 46022 Valencia, Spain
*sbnazars@iteam.upv.es

Abstract: A novel microwave frequency measurement scheme using a heterogeneous multicore fiber (MCF) is experimentally demonstrated. The inherently different relative group delays among the cores of a heterogeneous 7-core MCF are used to realize two individual 2-tap microwave filters with different free spectral ranges (FSRs). The ratio of the frequency response traces of these two filters is used to establish an amplitude comparison function (ACF). Furthermore, by varying the operational wavelength, the relative group delays between the cores and consequently the FSRs of the filters are tuned and different ACF curves are obtained. The complementary information provided by these different ACFs allows us to estimate the unknown frequency with an improved accuracy, over a broad measurement range. In our experiments, a measurement error of ±71 MHz is achieved over a frequency range of 0.5-40 GHz. The proposed scheme offers flexibility and compactness, thanks to the parallelism provided by the MCF.

1. Introduction

Accurate frequency measurement of an unknown microwave signal is essential for electronic warfare, anti-stealth defense and electronic intelligence systems [1,2]. It has also been identified as an element of interest for centralized radio access networks in fiber-wireless communications [3]. A frequency measurement receiver requires a wide operation bandwidth, high resolution and near real-time response. While conventional frequency measurement techniques in the electrical domain can obtain a high resolution, they have limitations in terms of their speed, bandwidth and vulnerability to electro-magnetic interference. These issues could be solved through using photonic-based frequency measurement approaches, as they offer broad bandwidth, high speed, immunity to electromagnetic interference and low loss [4,5].

Photonic-based frequency measurement is realized by mapping the unknown frequency to a parameter that could be easily measured, such as microwave or optical power [6–14] or time [15]. Frequency-to-power mapping has been demonstrated by using an optical comb filter [10], an optical mixing unit [16], or a dispersive delay element [6–9]. In the latter case, the dispersive element is used to either implement chromatic dispersion-induced microwave power fading [6–9] or realize a microwave photonic filter [17–19]. In both of these cases, a pair of frequency-dependent spectral responses, generated in two different channels, are often detected and their power ratio, referred to as amplitude comparison function (ACF), is used for the frequency estimation. Since the ACF obtained in a dispersive delay element has a periodic behavior, it enables a unique mapping between the measured power and the unknown frequency only when the measurement bandwidth is within a single monotonic interval of the ACF. For broader measurement bandwidths, however, each power measurement could correspond to several frequency solutions, making it difficult to accurately estimate the unknown frequency. Thus, due to the trade-off between the measurement bandwidth and the resolution, to avoid ambiguities, the measurement bandwidth is limited to one monotonic region of the ACF. To overcome this limitation and obtain a high resolution over a broad bandwidth, multiple ACFs could be jointly employed to determine the unknown RF frequency unambiguously beyond a single monotonic

#463152 https://doi.org/10.1364/OE.463152
Journal © 2022 Received 4 May 2022; revised 23 Jun 2022; accepted 23 Jun 2022; published 11 Jul 2022

Optics EXPRESS

region of the ACF [20–22]. In this case, thanks to the complementary information provided by the additional ACFs, the correct frequency solution can be picked out from the possible solutions.

In this paper, we present a microwave frequency measurement scheme using a heterogeneous multicore fiber (MCF). Such fibers have found applications in Microwave Photonics, due to their capability to operate as tunable optical sampled true-time delay lines, through exploiting the relative time delays between the cores [23,24]. Microwave photonics signal processing in multicore fibers is advantageous as they offer increased compactness due to their inherent parallelism, as well as performance flexibility and versatility. Moreover, MCFs have the capability of providing fiber-distributed signal processing without resorting to a dedicated system external to the fiber, which is particularly attractive in the context of radio access networks for 5G and Beyond. In our proposed scheme, multiple ACFs are obtained, making it possible to retrieve the unknown RF frequency with a high resolution over a large bandwidth. Each ACF is the ratio of the frequency responses of two microwave photonic filters with different free-spectral ranges, where each filter is constructed using two cores of the heterogeneous multicore fiber. Compared to previous reports using several ACF curves [20–22], our scheme offers a simpler structure with less number of modulators and photodetectors and is more compact as only one spool of MCF is used. Moreover, both the measurement range and resolution are adjustable.

2. Working principle

Our proposed frequency measurement scheme using a heterogeneous multicore fiber is depicted in Fig. 1. A continuous-wave laser is modulated by an intensity modulator (IM), driven by an unknown microwave signal. The modulated optical signal is then launched into four cores of a heterogeneous MCF, which have distinct dispersive properties. Two cores are combined using a coupler, while the other two cores are combined using another coupler and the output of the couplers are detected separately by a pair of photodetectors (PD). In the context of radio access networks, this scheme could be used for remote frequency measurement between a base station and a remote antenna unit, by placing the modulator in the remote unit and the other equipment in the base station. In this case, if the MCF link is long enough, an additional core (different from the previously mentioned cores) could be used to transmit the continuous-wave signal from the laser in the base station to the remote unit, and the aforementioned four cores could be used to transmit the modulated signal back to the base station. Thus, the MCF could be simultaneously used for the transmission of the signal and for the measurement of the unknown frequency.

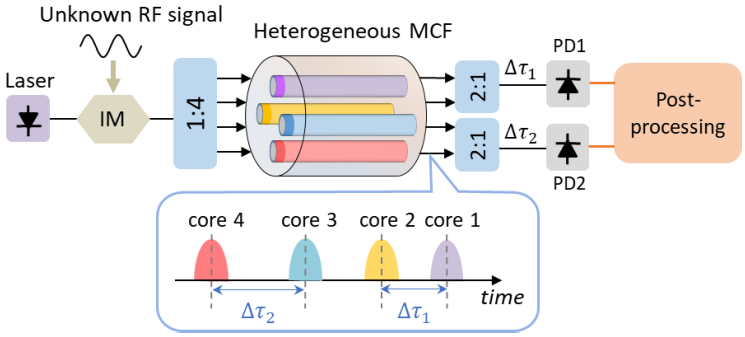

Fig. 1. Schematic diagram of the proposed microwave frequency measurement scheme using a heterogeneous multicore fiber. IM: intensity modulator, PD: photodetector.

After propagation through a given core n, the group delay, τ_n, at an optical wavelength λ, can be expanded in a first-order Taylor series around an anchor wavelength λ_0, as [23]:

$$\tau_n(\lambda) = [\tau_{0,n} + D_{0,n}(\lambda - \lambda_0)]L, \tag{1}$$

Optics EXPRESS

where $\tau_{0,n}$ and $D_{0,n}$ are the group delay per unit length and chromatic dispersion of core n at λ_0, respectively, and L is the fiber length. The differential group delay (DGD) between cores n and m, is then expressed as:

$$\Delta\tau(\lambda) = [\Delta\tau_0 + \Delta D(\lambda - \lambda_0)]L, \tag{2}$$

where $\Delta\tau_0 = \tau_{0,m} - \tau_{0,n}$ and $\Delta D = D_{0,m} - D_{0,n}$ are the differential group delay per unit length and differential chromatic dispersion between two cores at the anchor wavelength.

The DGD among the cores could be used to realize 2-tap microwave signal filters, through combining the output of any two cores and detecting them jointly with a single photodetector [5]. Thus, after propagation through the four heterogeneous cores, two individual 2-tap microwave signal filters could be implemented, where the DGD between the cores constructing the two filters are $\Delta\tau_1$ and $\Delta\tau_2$, respectively. The microwave power, P_j, detected at the output of filter j, $(j = 1, 2)$ can be written as

$$\mathrm{P}_j \propto R_j[1 + \cos(2\pi f_{RF}\Delta\tau_j)] = 2R_j\cos^2(\pi f_{RF}\Delta\tau_j), \tag{3}$$

where f_{RF} is the unknown frequency of the microwave signal and the free spectral range (FSR) of filter j is $\mathrm{FSR}_j = 1/\Delta\tau_j$. The responsivity of the PD associated with each filter is represented by R_j. The ratio between the two detected powers is used as the ACF, given by

$$\mathrm{ACF} = \frac{P_1}{P_2} = \frac{R_1\cos^2(\pi f_{RF}\Delta\tau_1)}{R_2\cos^2(\pi f_{RF}\Delta\tau_2)}. \tag{4}$$

To get a better understanding, the frequency responses of two 2-tap microwave filters, with DGD values of 100 ps and 200 ps are shown in Fig. 2(a), while their power ratio is the yellow curve depicted in Fig. 2(b). It can be seen that the ratio has a larger slope than the individual frequency responses; thus, using the power ratio to estimate the unknown frequency increases the measurement resolution. Moreover, as can be seen in Eq. (4), the ACF is not sensitive to the RF power and its possible variations. Also, since only one optical laser is used in our scheme, the measurement system is not influenced by the fluctuations of the laser power.

According to Eq. (4), there is a unique mapping between the ACF value and the RF frequency over a frequency range, determined by the smallest FSR_j or the largest $\Delta\tau_j$, $(j = 1, 2)$. Thus, within this frequency range, in which the ACF is monotonic, one can calculate the unknown RF frequency from the measured ACF. However, when the frequency measurement bandwidth is larger than a monotonic interval of the ACF, for a given power measurement, several potential frequency solutions are found (see the yellow and purple dots in Fig. 2(b)), making the identification of the correct solution unfeasible. Thus, on one hand, the ACF requires a large monotonic interval, to increase the frequency measurement bandwidth, and on the other hand, the measurement resolution becomes relatively low in large monotonic intervals. To overcome this trade-off and simultaneously increase the measurement bandwidth and resolution, one can use multiple ACFs instead of just one. The collective information provided by different ACFs can be used to determine the correct frequency solution.

In order to obtain several ACFs using our proposed scheme, we have taken advantage of the dependence of the DGD on the optical wavelength, as indicated by Eq. (2). By tuning the laser wavelength, $\Delta\tau_1$ and $\Delta\tau_2$ values change, and consequently we can get multiple ACFs. Moreover, it is also possible to increase the number of ACFs by constructing multiple (instead of just two) 2-tap microwave filters, using MCF cores with different $\Delta\tau$ values. However, this would require a higher number of photodetectors, i.e, two photodetectors per ACF. Therefore, we will restrict the number of microwave filters to 2.

To estimate the unknown frequency using our proposed scheme, initially, for several specific laser wavelengths (different $\Delta\tau$ values), the corresponding ACF values over a given microwave frequency bandwidth are found and stored in a look-up table. The look-up table, which expresses

Optics EXPRESS

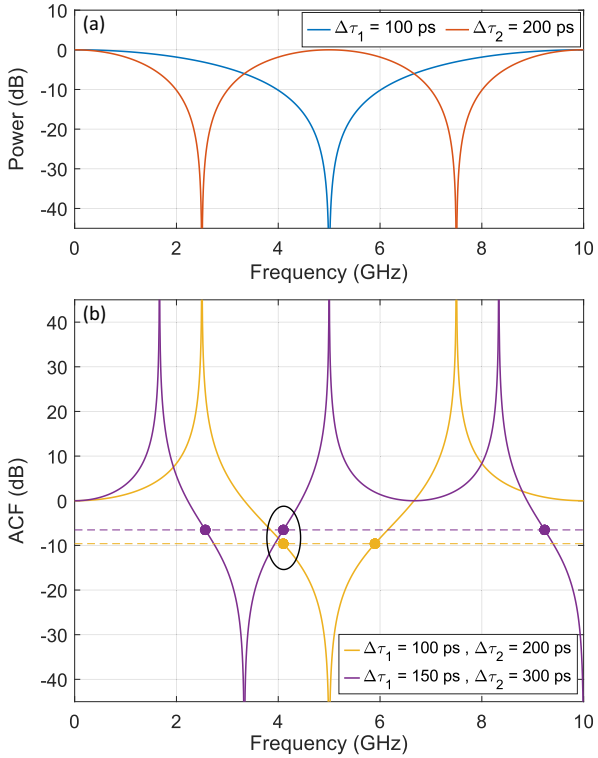

Fig. 2. (a) Simulated frequency responses of two 2-tap microwave filters with different FSRs. (b) Simulated ACF curves for 2 wavelengths, with different $\Delta\tau_1$ and $\Delta\tau_2$ values. The yellow and purple curves are referred to as ACF I and ACF II, respectively. ACF I is the power ratio of the two microwave filter frequency responses shown in (a). Dashed lines indicate the microwave power ratio corresponding to 4.1 GHz for each of the two ACF curves. The dots show all the frequencies of each ACF curve that have the same power ratio value as that of 4.1 GHz.

the relationship between each of the ACFs and the microwave frequency, is used as a reference. Then, after receiving an unknown microwave signal by the antenna, the powers at the output of the PDs are measured at those laser wavelengths and the corresponding power ratios are calculated. A search algorithm is used to compare the measured power ratio values with the look-up table and find all the potential solutions of each ACF. The intersection of the potential solutions of the different ACF curves is chosen as the unknown frequency. This is explained using a simulation in Fig. 2(b), where two ACF curves that are used to establish the look-up table, are displayed. In the yellow curve (ACF I), we have $\Delta\tau_1 = 100$ ps and $\Delta\tau_2 = 200$ ps, while in the purple curve (ACF II), it is assumed that the laser wavelength has changed and $\Delta\tau_1 = 150$ ps and $\Delta\tau_2 = 300$ ps are obtained. The yellow and purple horizontal dashed lines show the measured power ratios at a given unknown frequency, for ACF I and ACF II, respectively. The yellow and purple dots are, therefore, the potential frequency solutions of each ACF. The intersection of these solutions, which is 4.1 GHz, is estimated as the unknown frequency. It is worth mentioning that since there might be a small discrepancy among the solutions found by the two ACFs, the frequency found by ACF II should be used as the final estimated value, since it has a higher slope around 4.1 GHz as compared to ACF I.

In our simulations and experiment, two similar PDs are considered, leading to $R_1 = R_2$ in Eq. (4). Nevertheless, even if different PDs are employed, it will not affect the performance as

Optics EXPRESS

long as the look-up table is established using the same two PDs as the ones used later for the frequency measurements.

3. Heterogeneous multicore fiber

In this work, we use a 5-km dispersion-engineered heterogeneous MCF, with 7 trench-assisted cores placed in a hexagonal lattice structure. The MCF has GeO_2-doped silica cores (with different doping amounts and dimensions), that are surrounded by a pure silica inner cladding and a 1%-Fluorine-doped trench. More details about the fiber structure can be found in [24]. Originally, the cores of this MCF were designed and fabricated with the purpose of operating as tunable sampled true-time delay lines for applications in microwave photonics [23], which requires the DGD among any two neighboring cores to be constant and to vary linearly with the optical wavelength. According to Eq. (2), these conditions can be fulfilled when at the anchor wavelength, the group delay of all cores are identical ($\Delta\tau_0 = 0$) and ΔD among all neighboring cores is constant. To obtain $\Delta\tau_0 = 0$, we have used variable delay lines (VDLs) or suitable short lengths of single-mode fiber (SMF) to adjust the slight mismatches between the group delays of the cores at the anchor wavelength $\lambda_0 = 1530$ nm. Thereafter, since the cores are designed to have a constant ΔD among them, $\Delta\tau$ varies linearly with the optical wavelength and no further adjustment of the VDLs are required for operating at different wavelengths.

In Fig. 3, the designed and measured DGDs of the cores with respect to core 7 are displayed. A good agreement is observed between the theory and experimental measurements for cores 3 to 7, over a 30-nm wavelength range, which confirms that for any given wavelength within this range, the DGD is constant among neighboring cores (excluding cores 1 and 2). Cores 1 and 2, which are the two smallest cores, have been substantially affected by fabrication errors, which in turn has affected their dispersion properties and led to the mismatches observed between the theory and measurements. As can be seen, the DGD between cores 5 and 7 is twice that of cores 3 and 4. Accordingly, we have used the outputs of cores 3 and 4 and those of cores 5 and 7, to construct filters 1 and 2 of Fig. 1, respectively, where we have $\Delta\tau_2 = 2\Delta\tau_1$.

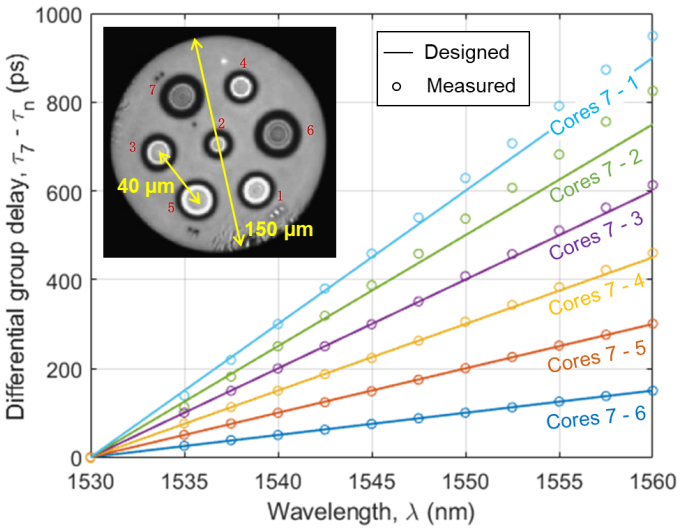

Fig. 3. Differential group delays of the MCF cores with respect to core 7. The inset shows the SEM image of the fabricated MCF.

Optics EXPRESS

The measured chromatic dispersion of cores 1 to 7 at 1530 nm are 14.4, 15.2, 16.6, 17.6, 18.6, 19.6 and 20.6 ps/km/nm, respectively, showing an incremental dispersion of ΔD = 1 ps/km/nm for cores 3 to 7.

4. Experiment and discussion

Figure 4 shows the frequency measurement experimental setup. A broadband source followed by a 0.1-nm-bandwidth optical filter is used as the input optical signal, in order to avoid optical coherent interference. The optical signal is amplified by an erbium-doped fiber amplifier (EDFA) and injected into an IM. The modulator is driven by a microwave signal generated by a Vector Network Analyser (VNA), where the RF power is 5 dBm and the RF frequency varies from 10 MHz up to 40 GHz. To avoid the carrier suppression effect, single sideband modulation is employed. The modulated signal is split and launched into cores 3, 4, 5 and 7 of the 7-core MCF using a fan-in device. The average insertion loss of the cores is 5.8 dB and the average crosstalk among the cores at the MCF output (including the fan-in/fan-out devices) is below -40 dB. At the output of the 5-km MCF, VDLs are used to compensate the mismatches between the core DGDs at the anchor wavelength λ_0 = 1530 nm, similar to Fig. 3. The output power of the cores are then equalized using variable optical attenuators (VOAs) to obtain uniform amplitude distribution. Cores 3 and 4 are combined and detected together by a 43-GHz PD, to realize a 2-tap filter. Similarly, cores 5 and 7 are used to construct another 2-tap filter with a different FSR, given that $\Delta\tau_2 = 2\Delta\tau_1$. The ratio of the power detected by these two PDs is used as the ACF. By sequentially setting the operational wavelength at 1550, 1552, 1557 and 1560 nm through adjusting the optical filter, $\Delta\tau_1$ values of 100, 110, 135 and 150 ps are obtained, respectively. These DGD values are calculated according to Eq. (2), using the dispersion values provided in Section 3 and considering $\Delta\tau_0 = 0$ at 1530 nm. The ACF curves are measured ten times at each of these four wavelengths and their averages are employed to establish a look-up table, as shown in Fig. 5.

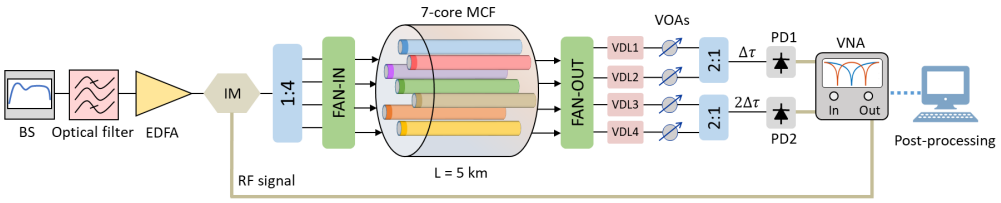

Fig. 4. Experimental setup of the proposed microwave frequency measurement scheme. BS: broadband source, EDFA: erbium-doped fiber amplifier, IM: intensity modulator, VDL: variable delay line, VOA: variable optical attenuators, PD: photodetector, VNA: vector network analyser.

To evaluate the performance of the proposed scheme in estimating unknown frequencies, the microwave frequency applied to the modulator is swept from 0.5 GHz to 40 GHz in 0.5-GHz steps and for each applied frequency, the operational wavelength is successively set to 1550, 1552, 1557 and 1560 nm. For each wavelength, firstly, the power detected by the two PDs is measured and their ratio is calculated. Secondly, using a search algorithm, the measured power ratio is compared with the look-up table (with the ACF curve of Fig. 5 corresponding to the same wavelength) and all the frequencies that have the same power ratio as the measured value are found and appointed as potential solutions of that ACF curve. The differences between the potential solutions found for the four ACF curves are calculated and the frequency with the minimum difference is estimated as the unknown frequency (see Fig. 5). Once the whereabouts of the unknown frequency are known, the final estimated value is chosen from the ACF curve

Optics EXPRESS

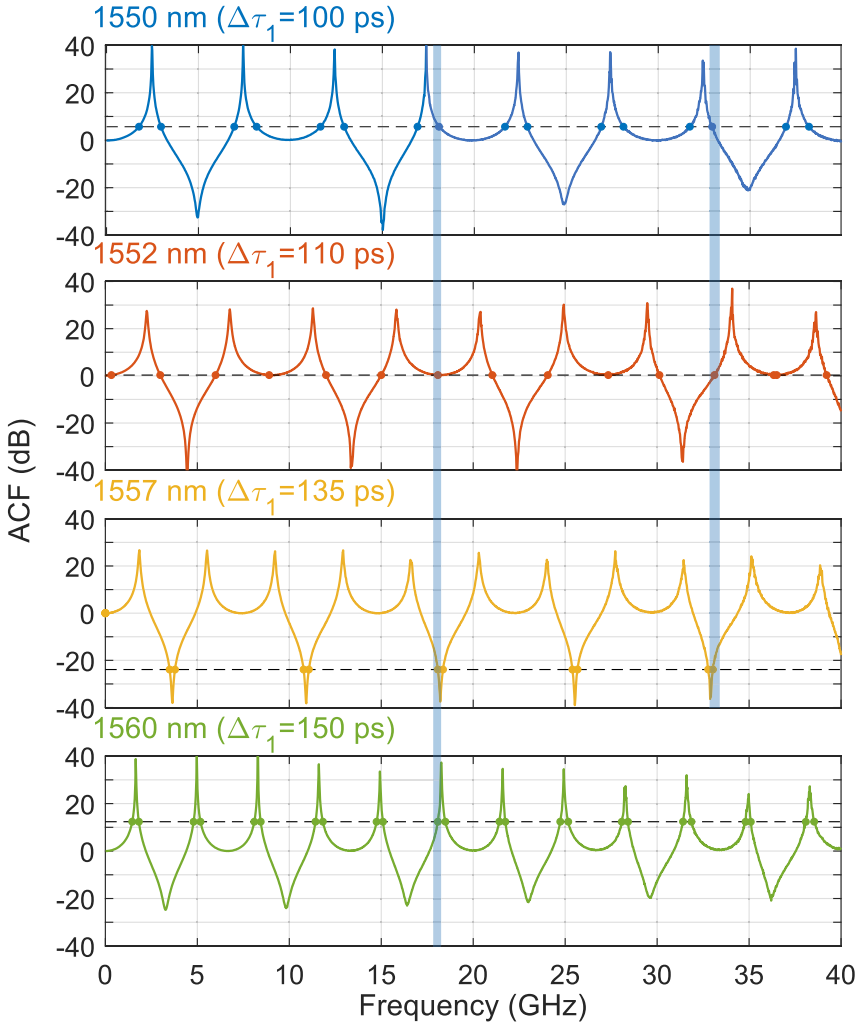

Fig. 5. ACF curves measured at four different wavelengths. The relative group delays between the cores used for implementing the two 2-tap filters are $\Delta\tau_1$ and $\Delta\tau_2$, respectively, where $\Delta\tau_2 = 2\Delta\tau_1$. The dashed lines indicate the microwave power ratio corresponding to 18 GHz for each of the ACF curves, while the dots show all the potential frequency solutions. As shown in the shaded areas, the first 3 ACF curves have a potential solution at both 18 GHz and around 33 GHz. However, while the fourth ACF curve has a solution at 18 GHz, it does not have one close to 33 GHz. Therefore, the unknown frequency should be estimated based on all 4 ACF curves, since using fewer curves could lead to considerable error.

that offers the best resolution, i.e. the one with the highest slope at that frequency (which in most cases, is the ACF curve with the largest $\Delta\tau$ value). Also, if a frequency is within the vague area close to the peaks or notches of an ACF curve, the value found by that curve is not used as the final frequency value.

It should be noted that since our measurement bandwidth is rather large (40 GHz), we need at least 4 ACF curves to be able to retrieve all the frequencies within this bandwidth with a small error. As explained in Fig. 5, if fewer number of ACF curves are used, there might be cases in which the intersection of the potential frequency solutions results in two frequencies instead

Optics EXPRESS

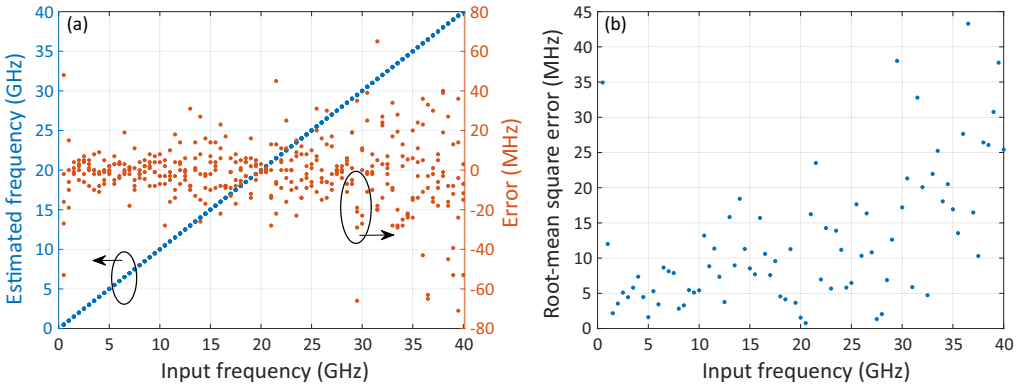

Fig. 6. (a) Estimated frequency as a function of the input frequency (blue dots) and the corresponding residual error (red dots). (b) The calculated root-mean square error at each input frequency.

of one, consequently leading to considerable measurement errors. Moreover, to considerably increase the measurement speed, one could use a multiport waveshaper and an ultrafast switch to switch between the 4 operational wavelengths.

Figure 6(a) displays the microwave frequency estimated by the proposed frequency measurement system versus the applied input frequency (in blue) along with the residual measurement error (in red), for five sets of measurements. The maximum residual error is below ±71 MHz and the root-mean square (rms) error, shown in Fig. 6(b), is below 44 MHz within 0.5-40 GHz. The larger error at higher frequencies could be related to their proximity to the bandwidth limit of the modulator and photodetector, which are both around 40 GHz. The sources that contribute to this error could be the amplified spontaneous emission noise of the EDFA, the bias drift of the IM, the shot noise and thermal noise from the PDs and the thermal noise of the VNA, which cause slight jitters in the notch frequency of the microwave photonic filters and consequently vary the ACF. Our results show a considerable improvement both in measurement bandwidth and resolution compared to previously reported frequency measurement schemes based on dispersive delay elements [7,8,17–22], which to the best of our knowledge in the best case had obtained errors of up to ±90 MHz over a 19.5-GHz frequency range [21]. Table 1 provides a comparison between our work and some other frequency measurement systems, in terms of their employed technology, measurement method and performance. In some studies exploiting optical nonlinearities, lower error microwave frequency estimations have been reported. A measurement error of 1 MHz over a range of 9-38 GHz has been achieved through stimulated Brillouin scattering (SBS) in a photonic chip [25], while four-wave mixing (FWM) in a highly nonlinear fiber (HNLF) has been used to obtain an error of 4.15 MHz within a 40-GHz bandwidth [26]. Although our measurement accuracy is not as good as these relatively more complex schemes based on optical nonlinear effects, we believe it is possible to further improve the accuracy of our scheme by increasing $\Delta\tau$ values and consequently increasing the slope of the ACF curves. This could be realized through different approaches, such as decreasing the anchor wavelength by adjusting the VDLs, increasing the length of the MCF, or using a different set of cores with larger DGDs to construct the microwave filters. For instance, cores 4 and 6 could be employed to realize one filter and cores 3 and 7 for another, which would double the $\Delta\tau$ values presented in this work.

As compared to using individual single-mode fibers, exploiting the multicore fiber assures a higher performance stability to environmental changes as all the optical paths are hosted by the same cladding, which reduces the possible variations in the DGDs between adjacent cores. Moreover, to avoid excessive measurement errors, different look-up tables corresponding to

Optics EXPRESS

Table 1. Comparison between different frequency measurement systems

Technology	Range (GHz)	Error (MHz)	Mapping type
SBS (chalcogenide chip) [25]	9-38	1	ACF
FWM (HNLF) [26]	0.04-40	4.15	Frequency-to-power
Micro-disk resonators [14] (silicon chip)	1.6-40	60	ACF
Dispersive element [21] (several SMF spools)	0.5-20	90	Multiple ACFs
Dispersive element (SMF) [9]	2-19	200	ACF
Frequency shifter + SBS (SMF) [15]	0.1-20	250	Frequency-to-time
FWM (silicon chip) [12]	0-40	318.9 (rms)	Frequency-to-power
Our work	0.5-40	71	Multiple ACFs

different environmental conditions could be established and according to the environmental conditions at the time of the frequency measurements, the correct associated look-up table could be used.

5. Conclusions

We propose and experimentally demonstrate, for the first time to our knowledge, a novel frequency measurement scheme based on a heterogeneous multicore fiber. The differential group delays between four cores of the multicore fiber are used to realize two tunable two-tap microwave filters with different free spectral ranges. The ratio between the frequency responses of these two filters is used to construct an amplitude comparison function. By tuning the wavelength of the signal propagating through the multicore fiber, the FSR of the filters is varied and different ACF curves are obtained. The unknown frequency is then estimated using the obtained ACFs. Within a measurement range of 0.5-40 GHz, a residual error of ±71 MHz (root-mean square error of 44 MHz) is achieved, which is a considerable improvement in terms of both measurement bandwidth and resolution as compared to previous reports based upon dispersive delay elements. This new demonstration extends the range of microwave signal processing applications enabled by a heterogeneous MCF.

Funding. European Research Council (Consolidator Grant Project 724663); Advanced Instrumentation for World Class Microwave Photonics Research (IDIFEDER/2018/031); Ministerio de Ciencia e Innovación (PID2020-118310RB-100).

Disclosures. The authors declare no conflicts of interest.

Data availability. Data underlying the results presented in this paper are not publicly available at this time but may be obtained from the authors upon reasonable request.

References

1. J. B. Y. Tsui, *Microwave Receivers with Electronic Warfare Applications* (Wiley, 1986).
2. D. L. Adamy, *Introduction to Electronic Warfare Modeling and Simulation; 1st ed.* (SciTech, 2006).
3. J. Capmany and P. Muñoz, "Integrated microwave photonics for radio access networks," J. Lightwave Technol. **32**(16), 2849–2861 (2014).
4. R. Minasian, "Photonic signal processing of microwave signals," IEEE Trans. Microw. Theory Techn. **54**(2), 832–846 (2006).
5. J. Capmany, J. Mora, I. Gasulla, J. Sancho, J. Lloret, and S. Sales, "Microwave photonic signal processing," J. Lightwave Technol. **31**(4), 571–586 (2013).
6. L. Nguyen and D. Hunter, "A photonic technique for microwave frequency measurement," IEEE Photonics Technol. Lett. **18**(10), 1188–1190 (2006).
7. X. Zou and J. Yao, "An optical approach to microwave frequency measurement with adjustable measurement range and resolution," IEEE Photonics Technol. Lett. **20**(23), 1989–1991 (2008).
8. J. Zhou, S. Fu, S. Aditya, P. P. Shum, and C. Lin, "Instantaneous microwave frequency measurement using photonic technique," IEEE Photonics Technol. Lett. **21**(15), 1069–1071 (2009).

Optics EXPRESS

9. X. Zou, S. Pan, and J. Yao, "Instantaneous microwave frequency measurement with improved measurement range and resolution based on simultaneous phase modulation and intensity modulation," J. Lightwave Technol. **27**(23), 5314–5320 (2009).
10. H. Chi, X. Zou, and J. Yao, "An approach to the measurement of microwave frequency based on optical power monitoring," IEEE Photonics Technol. Lett. **20**(14), 1249–1251 (2008).
11. S. Fu, J. Zhou, P. P. Shum, and K. Lee, "Instantaneous microwave frequency measurement using programmable differential group delay (DGD) modules," IEEE Photonics J. **2**(6), 967–973 (2010).
12. M. Pagani, B. Morrison, Y. Zhang, A. Casas-Bedoya, T. Aalto, M. Harjanne, M. Kapulainen, B. J. Eggleton, and D. Marpaung, "Low-error and broadband microwave frequency measurement in a silicon chip," Optica **2**(8), 751–756 (2015).
13. L. A. Bui, "Recent advances in microwave photonics instantaneous frequency measurements," Prog. Quantum. Electron. **69**, 100237 (2020).
14. Y. Chen, W. Zhang, J. Liu, and J. Yao, "On-chip two-step microwave frequency measurement with high accuracy and ultra-wide bandwidth using add-drop micro-disk resonators," Opt. Lett. **44**(10), 2402–2405 (2019).
15. T. A. Nguyen, E. H. W. Chan, and R. A. Minasian, "Instantaneous high-resolution multiple-frequency measurement system based on frequency-to-time mapping technique," Opt. Lett. **39**(8), 2419–2422 (2014).
16. L. A. Bui, M. D. Pelusi, T. D. Vo, N. Sarkhosh, H. Emami, B. J. Eggleton, and A. Mitchell, "Instantaneous frequency measurement system using optical mixing in highly nonlinear fiber," Opt. Express **17**(25), 22983–22991 (2009).
17. X. Zou, W. Pan, B. Luo, and L. Yan, "Dispersion-induced-loss-independent photonic instantaneous frequency measurement using remote-fiber-based tunable microwave filter," IEEE Photonics Technol. Lett. **22**(15), 1090–1092 (2010).
18. K. Xu, J. Dai, R. Duan, Y. Dai, Y. Li, J. Wu, and J. Lin, "Instantaneous microwave frequency measurement based on phase-modulated links with interferometric detection," IEEE Photonics Technol. Lett. **23**(18), 1328–1330 (2011).
19. Z. Zhao, K. Zhu, L. Lu, and C. Lu, "Instantaneous microwave frequency measurement using few-mode fiber-based microwave photonic filters," Opt. Express **28**(25), 37353–37361 (2020).
20. B. Vidal, "Photonic-based instantaneous microwave frequency measurement with extended range," Opt. Commun. **284**(16-17), 3996–3999 (2011).
21. N. Shi, Y. Gu, J. Hu, Z. Kang, X. Han, and M. Zhao, "Photonic approach to broadband instantaneous microwave frequency measurement with improved accuracy," Opt. Commun. **328**, 87–90 (2014).
22. C. Yang, L. Wang, and J. Liu, "Photonic-assisted instantaneous frequency measurement system based on a scalable structure," IEEE Photonics J. **11**(3), 1–11 (2019).
23. I. Gasulla and J. Capmany, "Microwave photonics applications of multicore fibers," IEEE Photonics J. **4**(3), 877–888 (2012).
24. S. García, M. Ureña, and I. Gasulla, "Demonstration of distributed radiofrequency signal processing on heterogeneous multicore fibres," in *Proceedings of 45th European Conference on Optical Communication (ECOC 2019)*, pp. 1–4.
25. H. Jiang, D. Marpaung, M. Pagani, K. Vu, D.-Y. Choi, S. J. Madden, L. Yan, and B. J. Eggleton, "Wide-range, high-precision multiple microwave frequency measurement using a chip-based photonic Brillouin filter," Optica **3**(1), 30–34 (2016).
26. H. Emami, M. Ashourian, and M. Ebnali-Heidari, "Dynamically reconfigurable all optical frequency measurement system," J. Lightwave Technol. **32**(24), 4796–4802 (2014).